13th Australasian Fluid Mechanics Conference
Monash University, Melbourne, Australia
13-18 December 1998

MODELLING VISCOUS FLOW AROUND 2-D YACHT MAST AND SAIL CONFIGURATIONS

Keith I. BAILEY[1], Peter S. JACKSON[2] & Richard G.J. FLAY[3]

Yacht Research Unit
Department of Mechanical Engineering
University of Auckland, Auckland, NEW ZEALAND

ABSTRACT

The paper outlines a viscous-inviscid interaction method which couples a potential flow analysis with integral boundary layer calculations to determine the aerodynamic loads on two-dimensional yacht rig configurations. Results are validated for the foresail, and preliminary findings for the mast and mainsail are presented.

INTRODUCTION

The ability to predict the performance of a yacht is an invaluable and relatively inexpensive way of exploring the bounds of a complex design envelope. Sails and their aerodynamic characteristics are an integral part of such performance predictions. The ability to predict sail performance in turn requires a theoretical and practical understanding of the interaction of sails with the wind.

Milgram (1998) concluded that "the effect of the boundary layers on sail aerodynamics will almost certainly be incorporated in the numerical methods within a very few years. The degree to which these methods can accurately deal with the wake of the mast that then streams across the sail attached to it remains to be seen."

The research this paper describes is aimed at developing a viscous model for the flow about upwind 2-D yacht mast and sail configurations. Such flows are characterised by (refer to Figure 1):

(I) Laminar boundary-layer flow from stagnation on the mast and windward side of the foresail.
(IIa) A leading-edge separation bubble on the foresail.
(IIb) Separation bubbles from the rear of the mast with turbulent reattachment on the mainsail.
(III) Turbulent boundary-layer growth over the sails.
(IV) Possible turbulent separation ahead of the trailing edges.

No structural considerations of the sail are included in this model – the sail shape is fixed.

Milgram (1978) has performed water-tunnel tests and collated useful experimental data for aerodynamic loads over various combinations of wooden elliptic mast and bronze NACA 6-series mean-line (a=0.8) sail shapes. His sails had a parabolic thickness-form ratio of 0.034. He found that the drag of a mast/sail combination is not given by the sum of its separate drag components. He also noted that, for three-dimensional rig geometries, "the addition of a mast to a sail raises the sum of its form and friction drag to the same order of magnitude as the induced drag of that sail."

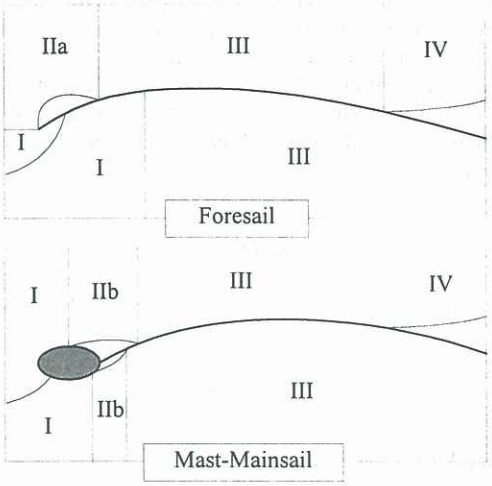

Figure 1: Regions around 2-D yacht rig configurations.

Wilkinson (1984) notes that the first published theoretical mast/sail combination study, due to Vaussy (1972), neglected the presence of separated regions and thus was restricted to flow cases of low incidence approaching streamlined masts, at negative mast angles, with small camber-ratio sails.

Wilkinson developed a potential flow method to describe a pseudo-viscous flow about a mast and sail combination. Although boundary layer effects were absent, the separated regions behind the mast and ahead of the trailing edge were simulated. Zero penetration was enforced along every surface while a constant tangential velocity was maintained within each separated flow portion. Comparing his experimental results with his partially separated flow theory, Wilkinson found that the theory failed to represent the pressure recovery adequately around the area of reattachment. He concluded from the experimental results that his potential flow boundary conditions within the bubble regions were erroneous -- the flow was neither tangential to the surface nor at constant pressure.

FEATURES OF THE MODEL

The model developed for the present study consists of several analytical or empirical modules that are contained within an overall, iterative framework for the viscous-inviscid interaction.

[1] Ph.D. Candidate, [2] Professor & HOD, [3] Assoc. Professor

Principles of Viscous-Inviscid Interaction

Viscous-inviscid interaction (VII) methods have emerged as a consequence of the nature of high Reynolds number flows. For most flows, viscous effects are confined within thin boundary layers, while the region external to the boundary layer can be considered as essentially inviscid. Thus separate calculation methods can be employed to solve for each flow region. The crux of VII is the interactive reconciliation of the two flow regimes. The classical interaction technique (see Figure 2) alters the inviscid flow boundary conditions to reflect the growth of the displacement thickness, δ^*, in the viscous boundary layer. In turn, the growth of the boundary layer is governed by the external, inviscid, streamwise-velocity distribution (dU_e / ds) impressed upon it. A composite flow solution is obtained from the successive iteration of the VII cycle, subject to some convergence criteria.

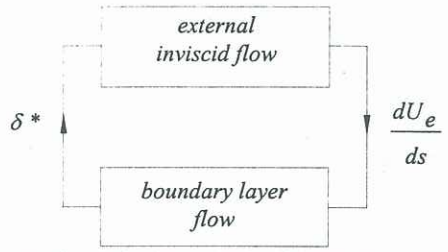

Figure 2: Classical viscous-inviscid interaction cycle.

Inviscid Flow Solution

The external inviscid flow is solved using panel method techniques, employing constant-strength source and doublet panels for the velocity potential due to the immersion of the mast and sail surfaces in a uniform flow. Mixed boundary conditions (internal Dirichlet/external Neumann) have been applied to minimise this perturbation potential. The singularity strengths are solved to ensure that a prescribed normal flow (V_N) exists at specific collocation points along the mast and sail surfaces.

Viscous and Inviscid Flow Matching

The reconciliation between the inviscid and viscous flow regions is achieved by matching primary flow quantities at a matching surface defined by discrete points in the flow. Application of Lighthill's (1958) surface transpiration concept allows the matching surface to be coincident with the airfoil surface. The traditional, zero penetration, surface boundary condition is replaced by a transpiration velocity obtained interactively from a current viscous solution.

Mast-Mainsail Separation

The bluff body separation and wake from the mast is modelled in a partially separated manner. The assumed bubble shapes are defined by cubic-hermite interpolation from laminar separation on the mast to a specified point of reattachment on the mainsail. The bubble length is currently empirically determined from the backward facing step study of Adams & Johnston (1988). The surface separation and reattachment angles are also defined to complete the interpolation. The bubble surface is assumed to enclose a conserved massflow rather than defining the boundary of reversed flow region. The mast and sail surfaces are altered to include these bubbles and the inviscid flow component is run sequentially with a laminar, integral boundary-layer method to ensure the correct mast separation points. Iteration is required to find a stable pair of bubble shapes.

Laminar Boundary-Layer Calculation

The boundary layers are calculated by integral methods. Thwaite's method is used for attached laminar flow. Transition to a turbulent boundary-layer may either be forced, or freely occur due to instability or separation.

Leading-Edge Bubble Model

A special case of transition occurs at the leading edge of the foresail. The laminar flow responds to the sharp leading edge corner by separating and forming a closed bubble after reattachment. The presence of the bubble serves to remove the negatively infinite inviscid pressure at the leading edge thus disallowing the generation of a leading edge suction force. Following conjecture that the flow field surrounding the leading edge separation bubble of a thin airfoil is a close facsimile of that about an airfoil with a rounded nose, then the tangential velocities either side of the sail are adjusted according to Lighthill's (1951) rule which depends on the leading-edge bubble radius and the distance from the leading edge. Jackson & Fiddes (1995) relate the bubble length, radius and turbulent reattachment momentum thickness to the square of the angle of departure from ideal incidence.

Turbulent Boundary-Layer Calculation

The integral method for calculating the growth of the turbulent boundary-layer is that due to Head. No second-order curvature or wake effects are considered. Modified empirical relations for the entrainment and skin-friction coefficients and the boundary layer shape factors are applied from the work of Jackson & Fiddes. Turbulent integration proceeds over the surfaces representing the mast-mainsail bubbles with zero skin-friction, and then continues along the mainsail. Turbulent trailing-edge separation is monitored and if detected, inverse boundary-layer calculations (due to Catherall & Mangler, 1966) are initiated to avoid the Goldstein singularity encountered by the traditional direct method at separation. In an inverse mode, the integral method is supplied with the equivalent source strength ($S = V_N / U_e$) and solves for the external velocity gradient (dU_e / ds).

The classical VII scheme represented by Figure 2 is suited for attached flow only. The presence of separated regions requires a stronger nature of interaction. In these regions, this study employs Carter's (1979) semi-inverse interaction method (Figure 3 overleaf), which is stable for attached, separating and separated flows.

Relaxation, Stability and Convergence

Once the current viscous solution has been resolved, the equivalent source strength distribution is relaxed by a factor deduced from a Fourier stability analysis of an approximate relationship between small perturbations in the velocity gradient and the equivalent source strength.

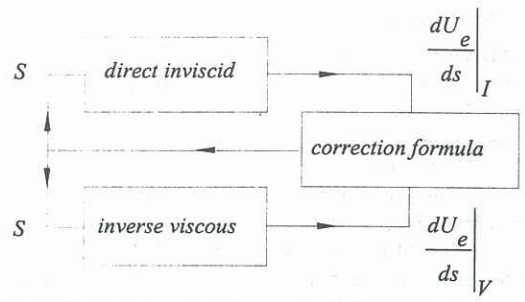

Figure 3: Semi-inverse viscous-inviscid interaction cycle

The relaxed equivalent source distribution provides the transpiration values required for the next inviscid flow calculation. This iterative interaction is continued until convergence of the inviscid panel speeds or the aerodynamic load coefficients is achieved. These loads are calculated by panel pressure summation.

VALIDATION OF THE FORESAIL MODEL

The current viscous model, when compared to that of Jackson & Fiddes, has a higher-order velocity potential representation, the ability to integrate through turbulent separated regions and an advanced VII relaxation scheme. The effect of these upgrades was assessed when both models were tested on a 10% cambered circular arc foresail. The Reynolds number representative of the flow was 1.8×10^6. The chordwise pressure coefficient distributions for this sail at apparent incidence angles of α=-5°, 4° and 6° are shown in Figure 4.

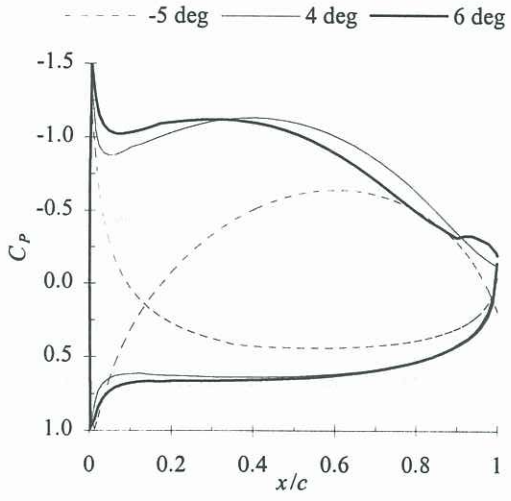

Figure 4: Pressure coefficient (C_p) vs. chordwise station (x/c) for 10% camber circular arc sail at Re=1.8×10^6

The relationship between the lift force coefficient and the apparent incidence angle is shown in Figure 5. Good agreement is achieved with Jackson & Fiddes in the range of -5° to 0°, where the leading-edge bubble is positioned on the concave side of the sail. The Jackson & Fiddes model predicts the presence of trailing-edge turbulent separation from 1° onward. Their model avoids the integration of such separated regions and extrapolates boundary-layer quantities from a point just before separation to the trailing edge. Uncertainty in these results is represented by using a dashed line. The current model, however, indicates that turbulent layer remains attached until 4°. Ideal incidence (the apparent incidence angle where no leading edge bubble is produced) is noted at 0.12°. Separated flow results are obtained for the incidence angle range of 6° to 8°. Converged results were not obtained between 4° and 6°. This was thought to be due a battle between the direct and semi-inverse schemes to control the relaxation of the equivalent source strengths.

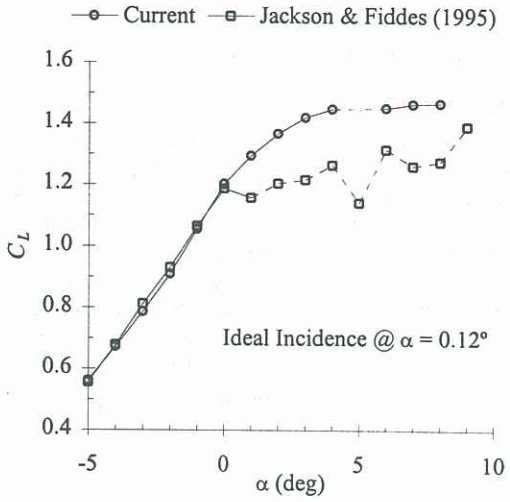

Figure 5: Lift force coefficient (C_L) vs. apparent incidence angle (α) for 10% camber circular arc sail at Re=1.8×10^6

The drag force coefficients calculated by each model are plotted against their respective lift force coefficients in the form of a polar diagram in Figure 6. The current model produces a smooth envelope. Minimum drag is obtained at the point of ideal incidence. Through the region of trailing edge separation ($\alpha > 4^\circ$) the lift remains approximately constant but the drag increases dramatically.

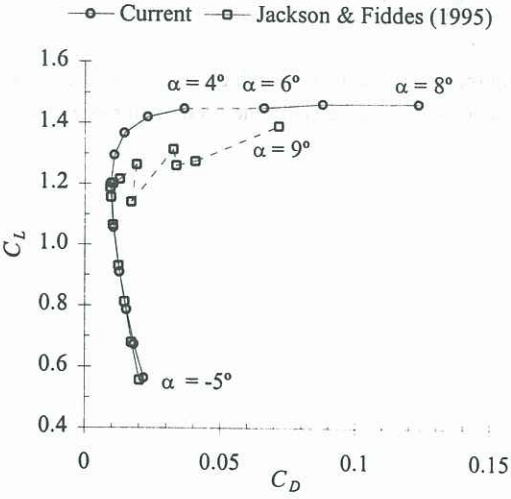

Figure 6: Lift force coefficient (C_L) vs. drag force coefficient (C_D) for 10% camber circular arc sail at Re=1.8×10^6

PRELIMINARY MAST-MAINSAIL RESULTS

Figure 7 shows the state of the boundary layer over a mast-mainsail configuration after the *first* viscous sweep. The incidence angle is 5° below the horizontal. The turbulent boundary-layer grows from the point of separation on the mast and is driven over the frictionless mast-mainsail bubble surface by the adverse pressure gradient alone. This results in a rapid thickening of the layer toward the point of reattachment. The primary effect of this interaction is to provide the mainsail with a greater "initial" thickness than it would have otherwise had if no mast had been present.

CONCLUSIONS

A viscous-inviscid interaction method for determining the aerodynamic loads over two-dimensional inelastic sails in viscous flow has been developed by coupling a potential flow analysis with integral boundary-layer techniques. It has been demonstrated for a circular arc "sail" that the lift force remains approximately constant and the drag increases considerably once trailing edge separation occurs. The minimum drag condition is obtained at ideal incidence. This method can be extended to cope with the flow about mast-mainsail combinations.

REFERENCES

ADAMS, E.W. & J.P. JOHNSTON, "Effects of the separating shear layer on the reattachment flow structure. Part 2: Reattachment length and wall shear stress", *Experiments in Fluids*, **6**, 493-499, 1988

CARTER, J.E., "A New Boundary-Layer Inviscid Interaction Technique for Separated Flow", *AIAA* Paper 79-1450, 45-55, 1979.

CATHERALL, D. & K.W. MANGLER, "The integration of the two-dimensional laminar boundary-layer equations pasts the point of vanishing skin friction", *J. Fluid Mech.*, **26**, 163-182, 1966.

JACKSON, P.S. & S.P. FIDDES, "Two-dimensional viscous flow past flexible sail sections close to ideal incidence", *Aero. J.*, **99**, 217-225, 1995.

LIGHTHILL, M.J., "A new approach to thin aerofoil theory", *Aero. Q.*, **3**, 193-210, 1951.

LIGHTHILL, M.J., "On Displacement Thickness", *J. Fluid Mech.*, **4**, 383-392, 1958.

MILGRAM, J.H., "Effects of Masts on the Aerodynamics of Sail Sections", *Marine Tech.*, **15**, 35-42, 1978.

MILGRAM, J.H., "Fluid Mechanics for Sailing Vessel Design", *Annual Rev. Fluid Mech.*, **30**, 613-653, 1998.

VAUSSY, P., "Etude d'une Voile Bidimensionnelle Inextensible en Presence d'un Mat", *Int. Shipbuilding Prog.*, **19**, 372-384, 1972.

WILKINSON, S., "Partially Separated Flow around 2-D Masts and Sails.", PhD Thesis, Ship Science Dept., University of Southampton, 1984.

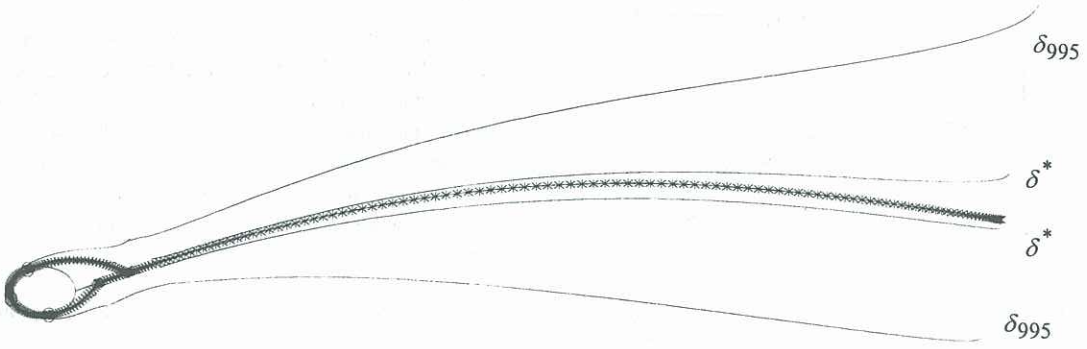

Figure 7: Boundary layer edge (δ_{995}) and displacement thickness (δ^*) over mast and sail configuration at end of first viscous sweep (scaled ten times in direction of the outward surface normal).